STRAIN CALCULATIONS FOR CIRCUMFERENTIAL GRABEN ON ALBA MONS, MARS. T. Öhman and P. J. McGovern, Lunar and Planetary Institute, Universities Space Research Association, 3600 Bay Area Blvd., Houston, TX 77058, USA. (ohman@lpi.usra.edu, mcgovern@lpi.usra.edu)

Introduction: Alba Mons (AM, previously Alba Patera) is a very shallow shield volcano on the northern slope of Tharsis rise, Mars (40ºN 250ºE; Fig. 1) [*e.g.,* 1–3]. It has a diameter of ~1400 km (E–W) × ~1000 km (N–S) km, but a relief of only ~7 km, making it distinctly different from the other volcanoes in the Tharsis region. Alba Mons is characterized by zones of circumferential graben located on the mid-flank of the volcano; wider Tantalus Fossae (TF) located lower on the more steeply sloping E flank, and narrower but more distinctly arcuate Alba Fossae (AF) higher up on the gently sloping W and the steepest NW flanks (Figs. 1–2). North of AM both AF and TF graben turn NE and continue to the lowlands. In the S, Tharsis-radial N–S-trending Ceranius Fossae (CF) graben extend to the S flank of AM (Fig. 1). The majority of AF and TF faults, and a part of CF, were formed during the Early Amazonian [4], with the circumferential faults postdating the radial ones [5].

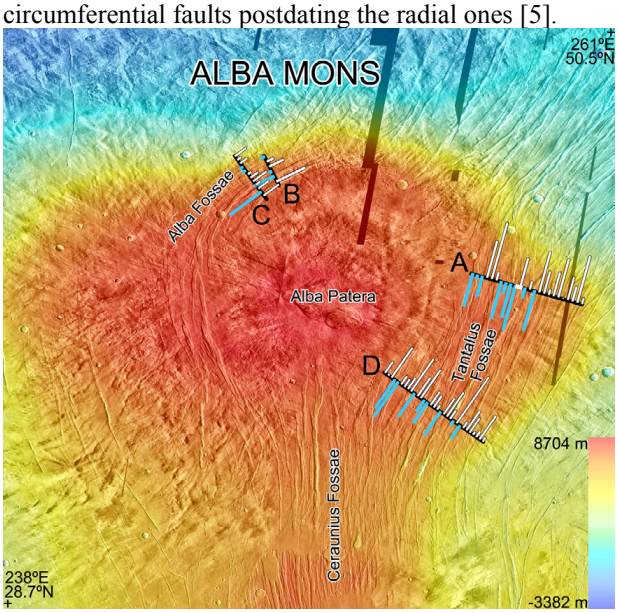

Fig. 1. Alba Mons (40ºN 250ºE) with the locations of topographic profiles. Individual profiles were taken perpendicularly to the graben and normal faults close to the main profile. White-in-black bars show the approximate location of graben (and normal faults) where outward throw is larger than inward (with bar heights indicating the relative amount of throw difference), blue bars showing the opposite. White dot shows the location of profile A5 in Fig. 3. MOLA DEM plotted on THEMIS day IR mosaic. Width of view ~1100 km.

Numerous models have been suggested for the formation of the circumferential graben, including regional faults splaying around a solidified pluton [2], only volcanic load [6], volcanic load superposed on a regional extensional stress field [7–8], a combination of lava loading, ceased dynamic support of endogenic activity, and contraction of the AM interior [9], loading stresses or increased crustal strength associated with plutonism [4], reservoir deflation and later volcanic loading [10–11], emplacement of sill complexes with bottom loading providing broader uplift [12], convective removal of a lithospheric root [13], cooling and shrinking volcanic core in the presence of a regional stress field [5], and long-lived multi-stage evolution mainly due to regional stresses (TF) and a response to the loading of the summit dome on the summit plateau and to the solidification of the magma reservoir (AF) [3]. In this study we have utilized various topographic datasets to gain further insight into the tectonic evolution of Alba Mons, particularly the circumferential graben, and to provide constraints for future modeling.

Data and methods: We used a number of topographic datasets in ESRI's ArcGIS 10.0 to get as representative and unbiased view of the fault topography in Alba Mons as possible. The datasets include MOLA points and digital elevation model (DEM, 128 px/degree, ~350 m/px [14–15]) and different DEMs derived from stereo imagery. High-Resolution Stereo Camera (HRSC) DEMs produced by the German Aerospace Center (DLR) were the most extensively used dataset (75–150 m/px) [16–17]. These were complemented by higher-resolution DEMs produced with the NASA Ames Stereo Pipeline (ASP) 1.0.5 software [18–19], using images from HRSC stereo channels and Mars Reconnaissance Orbiter Context Camera (CTX) stereo pairs, where available. Raw images were first processed with USGS ISIS 3.3.0, and bundle adjustment was not applied. THEMIS 100 m/px IR daytime mosaic, as well as the HRSC and CTX images were used for photogeologic reference.

Four profiles across the circumferential graben and normal faults on the flanks of Alba Mons have been measured (Fig. 1); two on the NW (profiles B and C, 65 and 97 km, respectively), one on the E (profile A, 204 km), and one on the SE flank (profile D, 233 km). Profile locations were selected based on the presence of prominent circumferential faults and the availability and quality of DEMs. We tried to assess the most reliable available dataset for each fault based on comparison between MOLA points, different DEMs, and imagery. As the graben are often highly asymmetric, apparent throws were measured separately for the outward- and inward-facing graben-bounding faults. For

the calculation of horizontal extension, we assumed a 60º fault angle: extension = apparent throw / tan 60º. Total extensional strains along the length of the profiles were calculated as: strain = Σheave / (profile length – Σheave). As the calculations are based on apparent throws, which is less than the original throw due to erosion, sedimentation, and profiles not always being exactly perpendicular to strike, the calculated extension and strain should be considered as minima.

Results and discussion: Apparent throws of 124 faults have been measured from the four profiles. The circumferential graben are highly complex [20] and often distinctly asymmetric, particularly closer to the summit (Figs. 2–3) [20–21]. The largest apparent throws of >600–700 m are found in the uppermost outward-facing graben-bounding faults in the NW profiles (Fig. 2). Almost as large apparent throw is found in profile A, but in the uppermost inward-facing fault (Fig. 2). In contrast, in the SE profile D the maximum apparent throw is only ~330 m, found both in the outward- and inward-facing faults. Locally the throw distribution varies between outward- and inward-facing faults (Fig. 3) and the situation commonly changes along the strike of the graben (see also [20]). There is a slightly increased tendency for the larger extension from inward-facing faults to be found in the upper parts of the profiles (Fig. 1). In all of the profiles total extension from the outward-facing faults is larger than from the inward-facing faults. The outward–inward difference in total extension is 200–300 m in profiles A–C, but >500 m in the longest SE profile D.

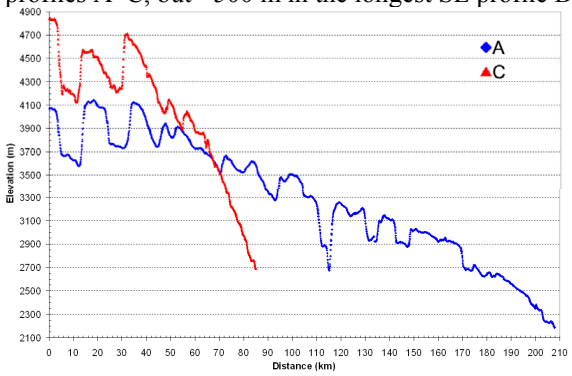

Fig. 2. Topographic profiles A (blue) and C (red) across Tantalus and Alba Fossae (Fig. 1), respectively, taken from mosaicked DLR HRSC DEMs. Note the asymmetry of the graben and the flanks. Vertical exaggeration ~49×.

Total strain in the eastern profile A is 1.63% (1.47% when CTX data are excluded), about twice the strain determined by [21] for a very similar profile on the eastern flank. The difference is probably mostly explained by our higher resolution data. The strain in our SE profile D is similar to profile A, 1.68%. These are somewhat less than in the two NW profiles, where strains are ~2%.

Conclusions: Alba Fossae accommodates more extensional strain (~2%) than Tantalus Fossae (~1.65%), further emphasizing the distinct structural E–W asymmetry [3, 12] of Alba Mons. The strain is also focused on the few graben closest to the summit (as also noted by, *e.g.,* [21]), particularly in Alba Fossae. The outward-facing faults produce more total extension than the inward-facing ones, which favors models with expansion and uplift [12] rather than contraction and subsidence. However, we tentatively note that the minor concentration of larger extension from inward-facing faults on the upper part of the flanks may imply a late phase of loading-related graben evolution. These data will be used to further constrain the tectonic evolution models of Alba Mons.

References: [1] Carr M. (1973) *JGR, 78,* 4049–4062. [2] Wise D. (1979) *Geologic Map of the Arcadia Quadrangle of Mars, Map I-1154,* USGS. [3] Ivanov M. and Head J. (2006) *JGR, 111,* E09003. [4] Tanaka K. (1990) *PLPSC 20,* 515–523. [5] Cailleau B. et al. (2003) *JGR, 108,* 5141. [6] Comer R. et al. (1985) *Rev. Geophys., 23,* 61–92. [7] Raitala J. (1988) *EMP, 42,* 277–291. [8] Turtle E. and Melosh H. (1997) *Icarus, 126,* 197–211. [9] Raitala J. and Kauhanen K. (1989) *EMP, 45,* 187–204. [10] Mège D. and Masson P. (1996) *PSS, 44,* 1499–1546. [11] Heller D.-A. and Janle P. (2000) *EMP, 84,* 1–22. [12] McGovern P. et al. (2001) *JGR, 106,* 23769–23809. [13] Scott E. and Wilson L. (2003) *JGR, 108,* 5035. [14] Zuber M. et al. (1992) *JGR, 97,* 7781–7797. [15] Smith D. et al. (1999) *Science, 284,* 1495–1503. [16] Gwinner K. et al. (2009) *PERS, 75,* 1127–1142. [17] Gwinner K. et al. (2010) *EPSL, 294,* 506–519. [18] Broxton M. and Edwards L. (2008) *LPSC XXXIX,* Abstract #2419. [19] Moratto Z. et al. (2010) *LPSC XXXXI,* Abstract #2364. [20] Schultz R. (2010) *JSG, 32,* 855–875. [21] Polit A. et al. (2009) *JSG, 31,* 662–673.

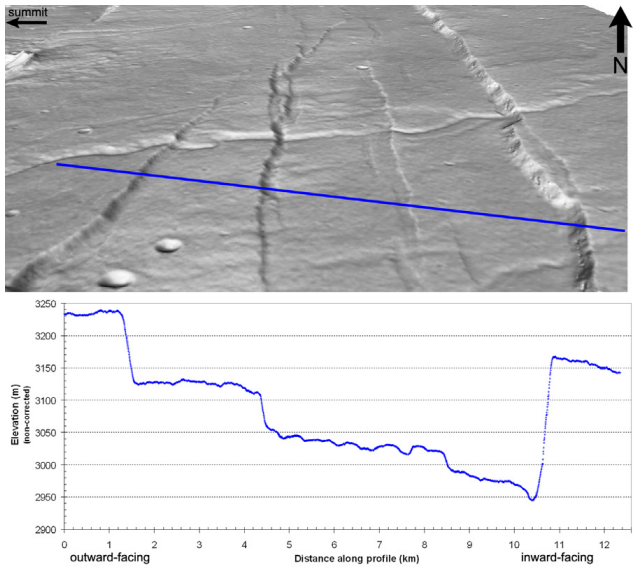

Fig. 3. Perspective view and a topographic profile A5 across a nested graben on the eastern flank of Alba Mons (see Fig. 1; ~40.8ºN 257.5ºE). In the outer graben the apparent throw is larger on the inward-facing fault, but in the inner graben the situation is reversed. Profile derived from a DEM produced with ASP [18–19] using CTX images G20_025970_2217_XN_41N102W.IMG and G20_025904_2209_XN_40N102W.IMG. Vertical exaggeration in the graph ~14×.